



CLICdp-Conf-2018-001
04 March 2022

Limits on top FCNC decay $t \rightarrow cH$ and $t \rightarrow c\gamma$ from CLIC at 380 GeV

A.F. Żarnecki^{1)*}, N. van der Kolk^{2)†}

On behalf of the CLICdp Collaboration

* Faculty of Physics, University of Warsaw, Poland, † Max-Planck-Institut für Physik, Munich, Germany

Abstract

FCNC top decays are very strongly suppressed in the Standard Model and the observation of any such decay would be a direct signature of physics beyond SM. Many "new physics" scenarios predict contributions to FCNC processes and the largest enhancement in many models is for $t \rightarrow cH$ decay. Enhancements for the decay channel $t \rightarrow c\gamma$ are more modest, but the decay still has a clearly identifiable kinematic signature. Prospects for measuring these decays at CLIC running at 380 GeV were studied with full detector simulation, taking the luminosity distribution, beam polarization and beam induced background into account. Top pair production events with $t \rightarrow cH$ decays can be identified based on the kinematic constraints and flavour tagging information. The analysis was divided into three steps: classification of top pair candidate events, event quality determination and kinematic reconstruction based on signal or background hypotheses, and final separation of signal from background. To obtain optimal results, selection criteria based on the dedicated Boosted Decision Trees (BDT) were used at each step. The expected limit on $\text{BR}(t \rightarrow cH) \times \text{BR}(H \rightarrow b\bar{b})$ from a combined analysis of hadronic and semi-leptonic top pair samples, as well as the limit on $\text{BR}(t \rightarrow c\gamma)$ from hadronic top pair decays are presented.

Talk presented at the International Workshop on Future Linear Colliders (LCWS2017), Strasbourg, France, 23-27 October 2017. C17-10-23.2.

© 2022 CERN for the benefit of the CLICdp Collaboration.

Reproduction of this article or parts of it is allowed as specified in the CC-BY-4.0 license.

¹Filip.Zarnecki@fuw.edu.pl

²now at Nikhef, Amsterdam, the Netherlands

1 Introduction

Top physics, together with Higgs boson studies and searches for Beyond the Standard Model (BSM) phenomena, is one of the three pillars of the research programme for future high energy e^+e^- colliders. As the top quark is the heaviest known elementary particle, with an expected value of the Yukawa coupling of the order of one, the precise determination of its properties is a key to understanding electroweak symmetry breaking. The determination of top properties is also essential for many “new physics” searches, as the top quark gives large loop contributions to many precision measurements that are sensitive to BSM effects. Stringent constraints on the new physics scenarios are also expected from direct searches for rare top decays. Both future linear colliders, the International Linear Collider (ILC) and the Compact Linear Collider (CLIC), provide an opportunity to study the top quark with unprecedented precision via direct production of thousands of $t\bar{t}$ pairs in e^+e^- collisions.

This contribution presents the prospects of constraining the branching ratio for the flavour changing top decays $t \rightarrow c\gamma$ and $t \rightarrow cH$ with CLIC running at $\sqrt{s} = 380$ GeV [1]. These decays are very strongly suppressed in the Standard Model with the expected branching ratios [2]:

$$\begin{aligned} \text{BR}(t \rightarrow c\gamma) &\approx 5 \cdot 10^{-14}, \\ \text{BR}(t \rightarrow cH) &\approx 3 \cdot 10^{-15}. \end{aligned}$$

At the same time a significant enhancement of these decays is expected in many extensions of the Standard Model, resulting from either the introduction of the direct tree level FCNC couplings or being due to the loop level contributions of new particles (or SM particles with modified couplings). For the $t \rightarrow c\gamma$ decay an enhancement up to the level of 10^{-5} is expected for some SUSY models with R -parity violation [3], while for the $t \rightarrow cH$ channel loop induced branching ratio of up to 10^{-4} is predicted in many models [4], with enhancement of up to 10^{-2} possible on the tree level [5]. Existing LHC constraints on the considered FCNC decays of the top quark are rather weak, at the level of $2 \cdot 10^{-3}$ [6–8] and the expected limits from HL-LHC are of the order of $2 \cdot 10^{-4}$ [2, 9]. Measurements at CLIC can be competitive for these channels thanks to the large sample of produced top quarks, clean environment and well constrained kinematics. The observation of any such decay would be a direct signature for “new physics”.

2 Event simulation and reconstruction

Detailed detector level analysis was performed for e^+e^- collisions at CLIC at $\sqrt{s} = 380$ GeV. With the assumed luminosity of 500 fb^{-1} and electron beam polarisation of -80% about 400 000 top quark pairs are expected. Dedicated signal samples were generated with WHIZARD 2.2.8 [10, 11]. For the $t \rightarrow c\gamma$ channel the model with anomalous top couplings (`SM_top_anom`) with vector type tensor $tc\gamma$ coupling was used while for the $t \rightarrow cH$ channel the simulation was based on the 2HDM(III) model implemented in SARAH [12]. For both models the parameter values were tuned to obtain a FCNC branching ratio of 10^{-3} so that the contribution from events with two FCNC decays is negligible. Detailed beam spectra for CLIC as well as beam induced backgrounds and the assumed electron beam polarization were taken into account. Generated events were passed to PYTHIA 6.4 for hadronisation with quark masses and other settings adjusted to the configuration used previously in CLIC CDR studies [13]. Signal samples were then processed with a standard event simulation and reconstruction chain of the CLICdp collaboration using the CLIC_ILD_CDR500 detector configuration. The background sample considered in the presented analysis included a full set of six-fermion event samples originally produced for CLICdp studies of top pair production at $\sqrt{s} = 380$ GeV. All sub-samples corresponded to an integrated luminosity of at least 500 fb^{-1} .

Analysis of the two top decay channels presented in this contribution was based on the so-called particle flow reconstruction performed using PANDORAPFA [14–16]. The reconstructed object collec-

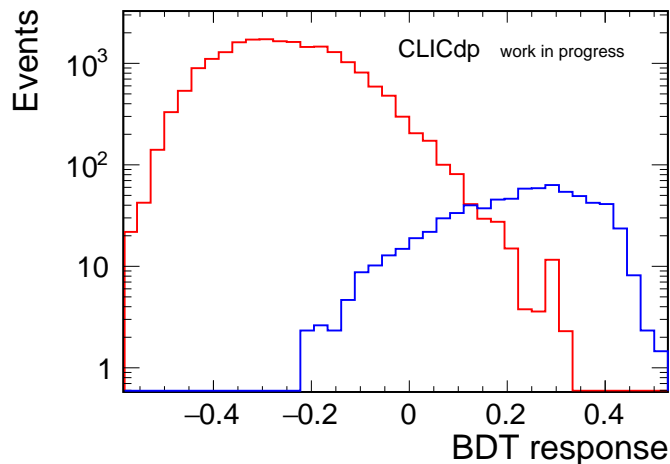


Figure 1: Distribution of the BDT classifier response for events with FCNC top decay $t \rightarrow c\gamma$ (signal, blue histogram) and SM top pair events (background, red histogram), for FCNC selection at 380 GeV CLIC. The background sample is normalised to 500 fb^{-1} and the assumed signal level corresponds to $\text{BR}(t \rightarrow c\gamma) = 10^{-3}$.

tion resulting from loose background rejection cuts [13] was used as an input for jet reconstruction with the Valencia algorithm [17] as well as for primary and secondary vertex reconstruction, and flavour tagging with LCFIPLUS [18].

3 $t \rightarrow c\gamma$ analysis

In this channel we search for top pair production events in which one of the top quarks decays into a charm quark and a photon. Due to the large top mass this decay results in a very striking signature: a high energy photon, with an energy of at least 50 GeV. Only the fully hadronic decay channel is considered where the second (spectator) top quark decays into a b-quark and a W-boson, which decays hadronically into two light quarks. The analysis requires that an isolated photon with an energy of at least 50 GeV is reconstructed in each selected event. This simple cut reduces the background from standard $t\bar{t}$ decays by a factor of 20 while keeping 92% of the signal events. Selected events are then subjected to kinematic fits, based on the jets reconstructed using the Valencia jet clustering algorithm, for both the signal ($\gamma + 4$ jets) and background (6 jet) hypotheses. The final selection of signal events is then based on a Boosted Decision Tree (BDT) algorithm, as implemented in the TMVA framework [19]. A total of 42 input variables were used to train the BDT, including photon properties, jet properties, flavour tagging information, invariant masses and χ^2 values from the kinematic fits. The distribution of the BDT classifier response for the considered signal (FCNC decay events) and background (SM top decays) samples is shown in Fig. 1. Shown in Fig. 2 is the reconstructed invariant mass distribution for the signal top quark, after the final selection cut based on the BDT response, $\text{BDT} > 0.2$. With this cut 60% of the signal events are selected while reducing the background contamination in the sample by a factor of about 500. The total selection efficiency resulting from the initial selection and BDT based selection is 55% for signal events and $9.4 \cdot 10^{-5}$ for $t\bar{t}$ background. Assuming the nominal integrated luminosity of 500 fb^{-1} collected at 380 GeV CLIC, the expected 95% C.L. limit on the top FCNC decay (assuming no signal contribution) is

$$\text{BR}(t \rightarrow c\gamma) < 3 \cdot 10^{-5}.$$

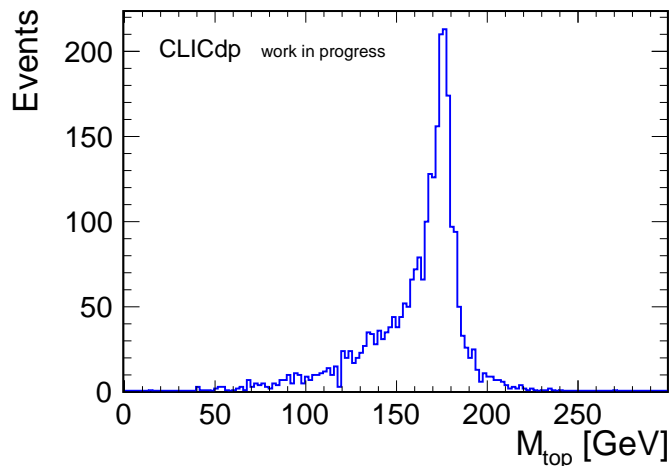


Figure 2: Invariant mass distribution of the top quark from the FCNC decay $t \rightarrow c\gamma$ reconstructed at 380 GeV CLIC after final selection cuts, for an integrated luminosity of 500 fb^{-1} and assuming $\text{BR}(t \rightarrow c\gamma) = 10^{-3}$.

4 $t \rightarrow cH$ analysis

The sensitivity of CLIC at 380 GeV to FCNC decay $t \rightarrow cH$ was studied for the dominant Higgs boson decay channel $H \rightarrow b\bar{b}$. Six jets are expected in the final state for top pair production events with one FCNC top quark decay and a hadronic decay of the second (spectator) top quark, while four jets, an isolated lepton and missing momentum are expected for events having a leptonic spectator decay. These final states have topologies that are compatible with the Standard Model top pair production events, which is therefore the dominant background contribution for this analysis. Discrimination between FCNC signal and SM top pair production events has to be based on the kinematic fit results and the flavour tagging information. For signal events we expect three jets in the final state to be tagged as b-quark jets (two from the Higgs boson and one from the spectator top quark decay) with two of them consistent with the invariant mass of the Higgs boson. A cut based approach, which was considered at the initial stage of the analysis [20], was found to be too inefficient for the considered process, as many observables had to be considered at the same time. This contribution presents the new analysis approach based on the use of multivariate analysis. BDT classifiers were used in the three analysis stages: classification of top pair candidate events (into hadronic, semi-leptonic and leptonic samples), estimation of the event reconstruction quality and the final signal-background discrimination.

For selection of hadronic and semi-leptonic event samples, two independent BDT classifiers, based on total event energy-momentum, event shape variables, isolated lepton information and jet reconstruction parameters were prepared. Only SM background samples were used for BDT training at this stage, with hadronic and purely leptonic top pair events used as a signal when training the hadronic and leptonic BDT classifiers respectively. Shown in Fig. 3 are the response distributions for these classifiers for different samples of top pair events. A cut on the hadronic BDT response was used to select the hadronic event sample, while a cut on both the hadronic and leptonic BDT responses was required for semi-leptonic event selection. Identification of the final state isolated lepton (electron or muon) was also required for the semi-leptonic events. The pre-selection based on the event classification included also the initial (loose) cut on the flavour tagging results: three jets were required to have a b-tag value of at least 0.4 and the fourth jet (jet coming from the c quark from FCNC decay) should have a sum of b-tag and c-tag values of at least 0.4.

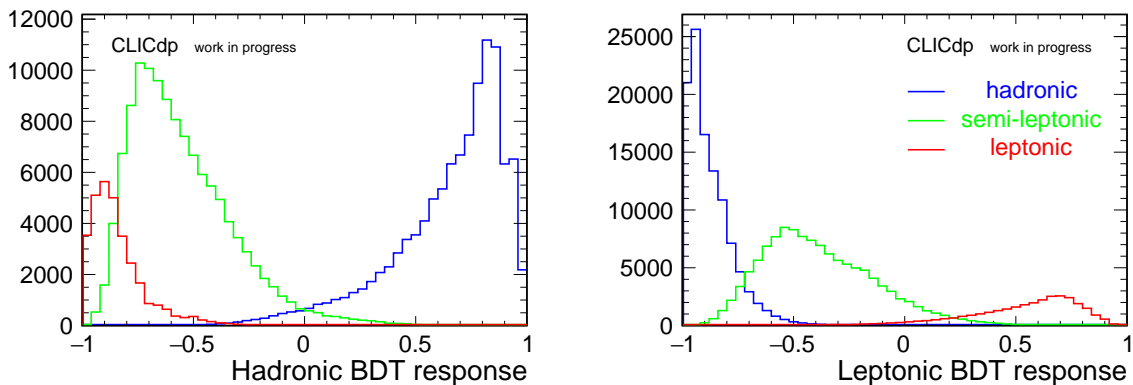


Figure 3: Response distributions for BDT classifiers trained to recognize hadronic top pair events (left) and leptonic top pair events (right), for different samples of $t\bar{t}$ SM background events, for 500 fb^{-1} at 380 GeV CLIC.

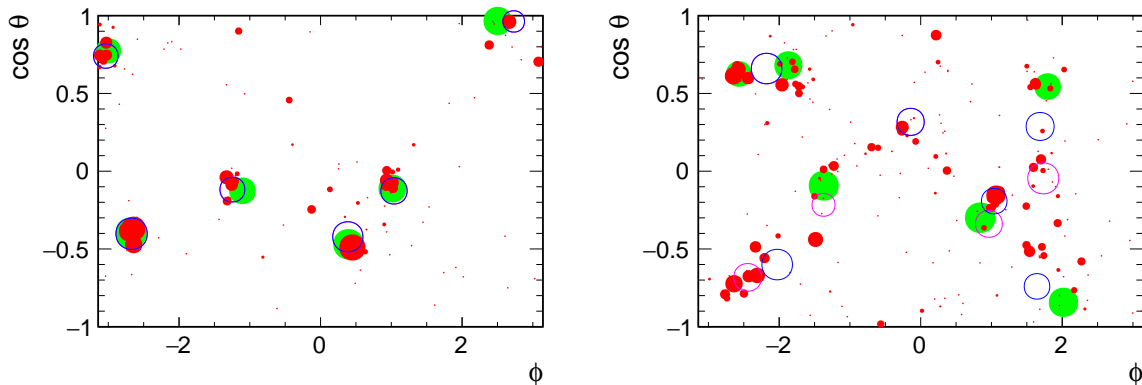


Figure 4: Schematic view of two SM top pair production events with fully hadronic final state. Directions in $(\cos \theta, \phi)$ of final state quarks (solid green circles) and reconstructed particle flow objects (solid red circles) are compared with clustering results of Valencia (open magenta circles) and anti- k_T (open blue circles) jet algorithms.

As mentioned above, the signal-background discrimination for $t \rightarrow cH$ channel has to be based on the kinematic fit results. However, the quality of the kinematic fit turned out to be very poor for a significant fraction of events, both for the signal and for the SM $t\bar{t}$ sample. Figure 4 shows two example top pair production events from the hadronic sample. Compared are the generator level directions of the final state quarks with the reconstructed particle flow objects and clustering results of Valencia algorithm (as used in the kinematic fit) and the anti- k_T jet clustering algorithms. For the majority of the events (as the one shown in Fig. 4 left), reconstructed jets correspond closely to the partonic final state on the generator level. For such well-reconstructed events a kinematic fit allows for precise determination of event kinematics and can be used for efficient discrimination between FCNC and SM top quark decays. However, for a significant fraction of events (like the one shown in Fig. 4 right) final state particles and the reconstructed particle flow objects do not follow the initial quark directions. This is mainly due to higher order QCD effects. The quality of the kinematic fit is very poor for such poorly reconstructed events and it cannot be used for efficient signal event selection. It is therefore important to try to discriminate

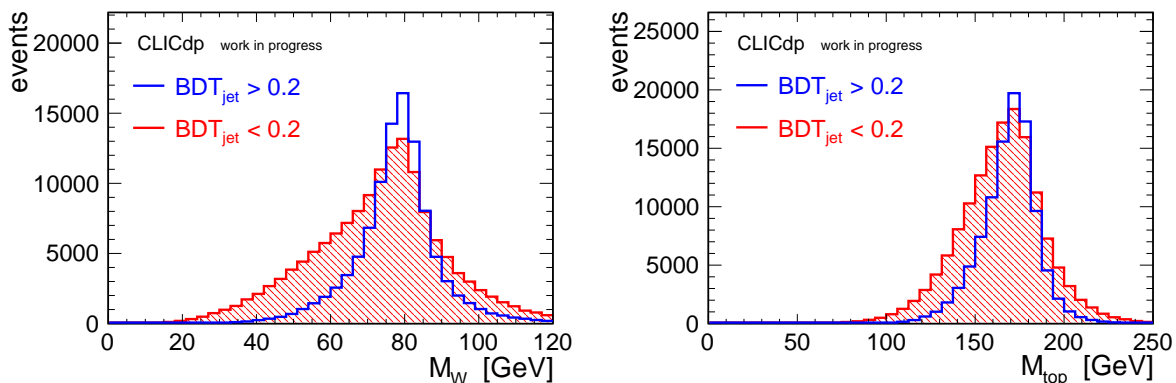


Figure 5: Influence of the cut on the event quality classifier response, BDT_{jet} , on the kinematic reconstruction of hadronic events. Reconstructed invariant masses of the W bosons (left) and top quarks (right) for SM top pair events (normalised to 500 fb^{-1}).

between well reconstructed and poorly reconstructed events.

The results of the kinematic fits should not be used to make any selection at this stage, as they will be used in the final step to discriminate between signal ($t \rightarrow cH$) and background ($t \rightarrow bW^+$) hypotheses. However, one can notice that for poorly reconstructed events the clustering results have a much stronger dependence on the clustering algorithm applied. It is therefore possible to estimate the event reconstruction quality by comparing results of different clustering algorithms. The BDT algorithm was trained separately for hadronic and semi-leptonic events using the angular distances and energy differences between jets reconstructed with three different jet algorithm configurations. The angular distance between the Valencia jets and the six-fermion final state on the generator level was used to define the reference samples for BDT training. The obtained event quality estimate (BDT response, BDT_{jet}) is only weakly correlated with the true parton-jet matching, but it does improve significantly the quality of kinematic reconstruction. Shown in Fig. 5 is the influence of the cut on the quality estimate on the reconstructed invariant mass of the W^\pm boson and the top quark, for the sample of hadronic $t\bar{t}$ events. The cut applied on the quality estimate significantly reduces the tails of the invariant mass distributions.

In the final step of the analysis, kinematic fits are performed for signal and background hypotheses. The jet combination which minimises the χ^2 value for the event is selected separately for each hypothesis. Flavour tagging results are used to reduce the number of possible configurations. Results from kinematic fits and the flavour tagging results are then used as an input for the final BDT selection optimised to discriminate between signal and background events. Resulting response distributions from the BDT classifiers trained to select signal events in hadronic and semi-leptonic samples are presented in Fig. 6. Final cuts on the BDT response were optimised to obtain the best expected limit on FCNC branching ratio, for the assumed luminosity of 500 fb^{-1} . The resulting cuts turned out to be relatively tight. The final selection efficiency for FCNC events is 10.4% while the background suppression is at the level of 10^{-4} . This results in the expected 95% C.L. limits of

$$\text{BR}(t \rightarrow cH) \times \text{BR}(H \rightarrow b\bar{b}) < 1.6 \cdot 10^{-4} \quad (1)$$

for 500 fb^{-1} collected at 380 GeV (hadronic and semi-leptonic samples combined). Details of the event selection efficiency for hadronic and semi-leptonic channel are presented in Tab. 1.

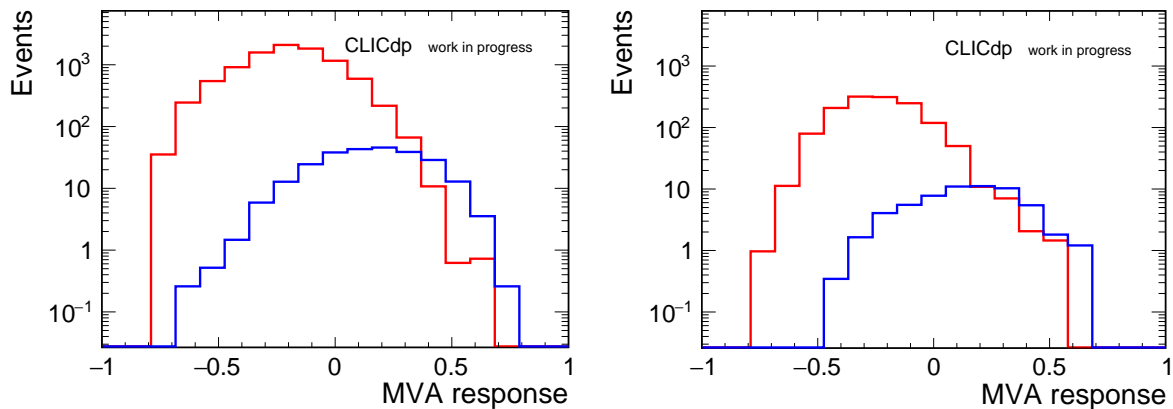


Figure 6: Response distribution of the BDT classifiers used for the final signal event selection for hadronic (left) and semi-leptonic (right) events. The background (red histogram) sample is normalized to 500 fb^{-1} while the signal (events with FCNC decay; blue histogram) to $\text{BR}(t \rightarrow cH) \times \text{BR}(H \rightarrow b\bar{b}) = 10^{-3}$ for the same integrated luminosity.

	Hadronic		Semi-leptonic	
	Signal	SM $t\bar{t}$	Signal	SM $t\bar{t}$
Classification	0.66	0.42	0.19	0.28
Flavour tagging	0.54	0.059	0.42	0.013
Event quality	0.89	0.90	0.92	0.90
Final MVA cut	0.23	0.0038	0.44	0.013
Total	0.072	0.000086	0.032	0.000044

Table 1: Summary of selection efficiency for analysis of the FCNC top quark decay $t \rightarrow cH$. Shown are the selected fractions of hadronic and semi-leptonic events, for FCNC signal and SM top pair production background, at different analysis stages as well as the total selection efficiency.

5 Conclusions

Considered in this contribution was the feasibility of measuring the FCNC top decay $t \rightarrow c\gamma$ and $t \rightarrow cH$ at CLIC running at 380 GeV. Results based on the full detector simulation were presented, taking luminosity distribution, beam polarization and beam induced background into account. For the $t \rightarrow c\gamma$ decay, based on the analysis of the hadronic channel only, the expected sensitivity (expected 95% C.L. limit on the FCNC branching ratio) is $3 \cdot 10^{-5}$, while for the $t \rightarrow cH$ decay the corresponding limit is $1.6 \cdot 10^{-4}$ (including Higgs branching ratio to $b\bar{b}$). Presented results should be considered as a “Work in Progress” report, the study is ongoing and publication of the final results is in preparation.

Acknowledgments

This work benefited from services provided by the ILC Virtual Organisation, supported by the national resource providers of the EGI Federation.

References

- [1] P. Burrows et al., eds., *Updated baseline for a staged Compact Linear Collider*, CERN, 2016, DOI: [10.5170/CERN-2016-004](https://doi.org/10.5170/CERN-2016-004).
- [2] K. Agashe et al., *Working Group Report: Top Quark*, Proc. Community Summer Study 2013: Snowmass on the Mississippi (CSS2013): Minneapolis, MN, USA, July 29-August 6, 2013, 2013, arXiv: [1311.2028](https://arxiv.org/abs/1311.2028) [hep-ph].
- [3] B. Mele, *Top quark rare decays in the standard model and beyond*, High energy physics and quantum field theory. Proceedings, 14th International Workshop, QFTHEP'99, Moscow, Russia, May 27-June 2, 1999, 1999, p. 224, arXiv: [hep-ph/0003064](https://arxiv.org/abs/hep-ph/0003064) [hep-ph].
- [4] S. Bejar, J. Guasch, J. Sola, *FCNC top quark decays beyond the standard model*, Proc. 5th Int. Symp. on Radiative Corrections - RADCOR 2000, 2001, arXiv: [hep-ph/0101294](https://arxiv.org/abs/hep-ph/0101294) [hep-ph].
- [5] L. Diaz-Cruz, C. Pagliarone, *Perspectives of detecting CKM-suppressed top quark decays at ILC*, Proc. Summer School and Conference on New Trends in High-Energy Physics: Experiment, Phenomenology, Theory, Yalta, Crimea, Ukraine, September 16-23, 2006, 2006, arXiv: [hep-ph/0612120](https://arxiv.org/abs/hep-ph/0612120) [hep-ph].
- [6] M. Aaboud et al., ATLAS, *Search for top quark decays $t \rightarrow qH$, with $H \rightarrow \gamma\gamma$, in $\sqrt{s} = 13$ TeV pp collisions using the ATLAS detector*, JHEP **10** (2017) 129, DOI: [10.1007/JHEP10\(2017\)129](https://doi.org/10.1007/JHEP10(2017)129), arXiv: [1707.01404](https://arxiv.org/abs/1707.01404) [hep-ex].
- [7] V. Khachatryan et al., CMS, *Search for top quark decays via Higgs-boson-mediated flavor-changing neutral currents in pp collisions at $\sqrt{s} = 8$ TeV*, JHEP **02** (2017) 079, DOI: [10.1007/JHEP02\(2017\)079](https://doi.org/10.1007/JHEP02(2017)079), arXiv: [1610.04857](https://arxiv.org/abs/1610.04857) [hep-ex].
- [8] V. Khachatryan et al., CMS, *Search for anomalous single top quark production in association with a photon in pp collisions at $\sqrt{s} = 8$ TeV*, JHEP **04** (2016) 035, DOI: [10.1007/JHEP04\(2016\)035](https://doi.org/10.1007/JHEP04(2016)035), arXiv: [1511.03951](https://arxiv.org/abs/1511.03951) [hep-ex].
- [9] ATLAS Collaboration, *Expected sensitivity of ATLAS to FCNC top quark decays $t \rightarrow Zu$ and $t \rightarrow Hq$ at the High Luminosity LHC*, ATL-PHYS-PUB-2016-019, 2016.
- [10] W. Kilian, T. Ohl, J. Reuter, *WHIZARD: Simulating Multi-Particle Processes at LHC and ILC*, Eur. Phys. J. **C71** (2011) 1742, DOI: [10.1140/epjc/s10052-011-1742-y](https://doi.org/10.1140/epjc/s10052-011-1742-y), arXiv: [0708.4233](https://arxiv.org/abs/0708.4233) [hep-ph].
- [11] M. Moretti, T. Ohl, J. Reuter, *O'Mega: An Optimizing matrix element generator*, 2001, arXiv: [hep-ph/0102195](https://arxiv.org/abs/hep-ph/0102195) [hep-ph].
- [12] F. Staub, *Exploring new models in all detail with SARAH*, Adv. High Energy Phys. **2015** (2015) 840780, DOI: [10.1155/2015/840780](https://doi.org/10.1155/2015/840780), arXiv: [1503.04200](https://arxiv.org/abs/1503.04200) [hep-ph].
- [13] L. Linssen et al., eds., *Physics and Detectors at CLIC: CLIC Conceptual Design Report*, CERN, 2012, DOI: [10.5170/CERN-2012-003](https://doi.org/10.5170/CERN-2012-003).
- [14] M. Thomson, *Particle Flow Calorimetry and the PandoraPFA Algorithm*, Nucl. Instrum. Meth. **A611** (2009) 25, DOI: [10.1016/j.nima.2009.09.009](https://doi.org/10.1016/j.nima.2009.09.009), arXiv: [0907.3577](https://arxiv.org/abs/0907.3577) [physics.ins-det].
- [15] J. Marshall, A. Münnich, M. Thomson, *Performance of Particle Flow Calorimetry at CLIC*, Nucl. Instrum. Meth. **A700** (2013) 153, DOI: [10.1016/j.nima.2012.10.038](https://doi.org/10.1016/j.nima.2012.10.038), arXiv: [1209.4039](https://arxiv.org/abs/1209.4039) [physics.ins-det].

-
- [16] J. S. Marshall, M. A. Thomson, *The Pandora Software Development Kit for Pattern Recognition*, Eur. Phys. J. **C75** (2015) 439, DOI: [10.1140/epjc/s10052-015-3659-3](https://doi.org/10.1140/epjc/s10052-015-3659-3), arXiv: [1506.05348](https://arxiv.org/abs/1506.05348) [[physics.data-an](#)].
- [17] M. Boronat et al., *Jet reconstruction at high-energy lepton colliders* (2016), arXiv: [1607.05039](https://arxiv.org/abs/1607.05039) [[hep-ex](#)].
- [18] T. Suehara, T. Tanabe, *LCFIPlus: A Framework for Jet Analysis in Linear Collider Studies*, Nucl. Instrum. Meth. **A808** (2016) 109, DOI: [10.1016/j.nima.2015.11.054](https://doi.org/10.1016/j.nima.2015.11.054), arXiv: [1506.08371](https://arxiv.org/abs/1506.08371) [[physics.ins-det](#)].
- [19] J. Therhaag, TMVA Core Developer Team, *TMVA: Toolkit for multivariate data analysis*, AIP Conf. Proc. **1504** (2009) 1013, DOI: [10.1063/1.4771869](https://doi.org/10.1063/1.4771869).
- [20] A. F. Żarnecki, CLICdp, *Sensitivity of CLIC at 380 GeV to the top FCNC decay $t \rightarrow cH$* , J. Phys. Conf. Ser. **873** (2017) 012049, DOI: [10.1088/1742-6596/873/1/012049](https://doi.org/10.1088/1742-6596/873/1/012049), arXiv: [1703.05007](https://arxiv.org/abs/1703.05007) [[hep-ex](#)].